World Journal of Advanced Research and Reviews
eISSN: 2581-9615 CODEN (USA): WJARAI
Cross Ref DOI: 10.30574/wjarr
Journal homepage: https://wjarr.com/

(RESEARCH ARTICLE)

Check for updates

Physics-based simulations applied to macromolecules: *Plasmodium falciparum* Dihydroorotate Dehydrogenase (6 VTY) in complexation with a series of pyrrole-derived inhibitors

Rika Justin Kouadja [1], Adama Niaré [1,*], Matthias Logbo Moussé [1], Ibrahim Bamba [1], Mamadou Guy-Richard Koné [2] and Eugène Megnassan [1,3,4,5]

[1] *Laboratory of Fundamental and Applied Physics, UFR SFA, Nangui Abrogoua University, BP 801 Abidjan 02, Côte d'Ivoire.*
[2] *Laboratory of Thermodynamics and Physico-chemistry of the Environment, UFR SFA, Nangui University 02 BP 801 Abidjan 02, Côte-d'Ivoire.*
[3] *Laboratory of Materials Science, Environment and Solar Energy, UFR SSMT, Félix Houphouët-Boigny University, BP 582 Abidjan 22, Côte d'Ivoire.*
[4] *Laboratory of Structural and Theoretical Organic Chemistry, Félix Houphouët-Boigny University, BP 582 Abidjan 22, Côte d'Ivoire.*
[5] *ICTP-UNESCO, QLS, Strada Costiera, 11, I-34151, Trieste, Italy.*

World Journal of Advanced Research and Reviews, 2025, 27(03), 961-972

Publication history: Received on 08 August 2025; revised on 14 September 2025; accepted on 16 September 2025

Article DOI: https://doi.org/10.30574/wjarr.2025.27.3.3231

Abstract

Despite the efforts and resources devoted to combating malaria, as well as the knowledge acquired about the different species of *Plasmodium*, of which Plasmodium falciparum is the most common in humans, malaria remains the leading endemic parasitic disease in the world. Malaria alone is responsible for approximately 597,000 deaths. It mainly affects pregnant women and children under the age of 5. The emergence of drug-resistant strains of the parasite poses a major challenge in the treatment of malaria. The enzyme dihydroorotate dehydrogenase (DHODH, pdb code: 6VTY) plays a crucial role in the treatment of malaria through the pyrimidine biosynthesis pathway, which is essential for the growth and reproduction of the Plasmodium falciparum (pf) parasite. Physics-based simulations applied to macromolecules are a major asset in the development of new drugs capable of overcoming resistance issues, improving selectivity, and increasing clinical efficacy. Using structure-based molecular design, we have developed Quantitative Structure-Activity Relationship (QSAR) models of 3D complexation from pyrrole (Pyl) molecule derivatives. A linear correlation has been established between Gibbs free energies (GFE: $\Delta\Delta G_{com}$) and the observed enzyme inhibition constants (IC_{50}^{exp}) for each complex formed: pIC_{50}^{exp} = - 0.1207×$\Delta\Delta G_{com}$+ 7.8526; R^2 = 0.95. The effect of the biological (aqueous) environment was taken into account as a component of $\Delta\Delta G_{com}$ through the free energy of molecular electrostatic solvation (ΔG_{sol}) solution of the Poisson-Boltzmann equation. The predictive power of the RQSA model was validated by the generation of 3D-RQSA Pharmacophores (PH4): pK_i^{exp} = 1,1585×pK_i^{pre} − 1.1448; R^2 = 0.93. The combination of 3D complexation and 3D-RQSA pharmacophore methodologies has provided key insights into the orientation and configuration of pyrrole (Pyl) molecules within the active site of dihydroorotate dehydrogenase (DHODH) for effective malaria control.

Keywords: QSAR Model; Complexation Model; Pharmacophore Model; Molecular Modeling; Dihydroorotate Dehydrogenase; Pyrrole Family

* Corresponding author: Niaré Adama

1. Introduction

Physics-based simulations have significantly increased the efficiency of computer-aided drug design (CADD). Molecular modeling (MM) and computer-aided combinatorial chemistry (CACC) have become new techniques for understanding many chemical, biological, and physical phenomena. These tools are increasingly useful for the pharmaceutical industry and enable the exploitation of natural substances [1]. The behavior of molecules can be simulated statically or dynamically [2]. This simulation includes, in particular, the behavior and flexibility of molecules during inhibition. The reaction mechanisms and interactions involved in enzyme catalysis are also included throughout this simulation [2]. Furthermore, physics-based simulation highlights complexation and the prediction of properties and functionalities based on structural analogies [2]. These techniques are proving to be essential in the development of new drugs to combat certain endemic diseases such as malaria, tuberculosis, HIV/AIDS, dengue fever, etc. These techniques are proving to be more than necessary in the development of new drugs to combat certain endemic diseases such as malaria, tuberculosis, HIV/AIDS, dengue fever, etc. In this paper, we focus on malaria due to the alarming statistics from the World Health Organization (WHO) [3]. Approximately 246 million people in 109 countries are exposed to malaria each year. Malaria remains the most significant parasitic disease, with more than 597,000 deaths, 77% of which are children under the age of 5 [3]. The situation has become a cause for concern because in most regions of the world, Plasmodium resistance has rendered traditional antimalarial drugs (quinine and chloroquine) ineffective, jeopardizing the fight against malaria [4]. Given this urgent need, the discovery and development of new therapeutic targets and new molecules are therefore required in order to expand the anti-malarial arsenal. Dihydroorotate dehydrogenase (DHODH), located in the mitochondria of the *Plasmodium falciparum* parasite and essential for its replication and development in red blood cells, is therefore an essential target for the treatment of malaria [5]. Pyrrole-based compounds are a diverse class of chemical compounds that target and block the activity of the enzyme dihydroorotate dehydrogenase (DHODH) [5]. In short, these pyrrole-based inhibitors play an essential role in the inhibition of DHODH [5]. The objective of this computer simulation work is to understand how pyrrole-based molecules interact within the active site of DHODH in order to evaluate the different binding forces that result. To achieve our objective, we developed a Quantitative Structure-Activity Relationship (QSAR) model based on DHODH-Pylx complexes obtained by in situ modifications of the crystallographic structure of the DHODH-Pyl1 complex [6, 7]. This model allowed us to establish a linear relationship between the relative change in Gibbs free energy of the formation of the DHODH-Pylx complex and inhibitory activities. This enabled us to identify the active conformation of Pylx at the active site of DHODH through complexation using Poisson-Boltzmann Molecular Mechanics (PB-MM). Using this active conformation, we created a 3D RQSA pharmacophore for DHODH inhibition.

2. Material and methods

2.1. Training and validation sets

In this work, the molecules used are from the pyrrole family. They have very interesting inhibitory properties in studies of dihydroorotate dehydrogenase (DHODH) enzyme inhibition. These pyrrole derivative molecules were synthesized and biologically evaluated by Sreekanth Kokkonda et al [7]. Their inhibitory potencies cover a wide range of inhibitory concentrations between 0.014 µM and 1.6 µM (Table 2), enabling the design of an RQSA model. Out of a total of 16 molecules, this pyrrole (Pyl) derivative inhibitors were divided into two groups comprising 12 for the test set and 4 for the validation set using the "Generation training and test set" protocol integrated into the Discovery Studio software [8].

2.2. Model construction

Three-dimensional (3D) models of free inhibitors (I), free DHODH enzyme (E), and enzyme-inhibitor complexes (E: I) were created based on the high-resolution crystal structure (1.18 Å) of a reference complex with the inhibitor Pyl 1 (PDB code: 6VTY) [7]. These models were generated using the graphical interfaces of the Insight-II [9] and Discovery Studio 2.5 [8] molecular modeling tools.

2.3. Molecular Mechanics

The modeling of DHODH and Pylx ligand complexes was performed using molecular mechanics, applying the CFF force field [10]. This process involves optimizing the geometry of ligand-enzyme interactions by minimizing energy, allowing for a more accurate representation of the binding and structural characteristics of the complexes.

2.4. Conformational search

The conformations of free inhibitors were derived from their bound conformations within protein-ligand (PL) complexes. This was achieved by implementing a stepwise relaxation process, allowing the structures to gradually adjust until they reached the nearest local energy minimum [11].

2.5. Solvation of Gibbs free energies

Ligand-receptor interactions occur in a solvent environment, which affects the binding process through hydrogen bonding and solvation effects. To account for these influences, the electrostatic component of Gibbs free energy was calculated by solving the nonlinear Poisson-Boltzmann equation [12], incorporating ionic strength. This equation can be written as:

$$\nabla^2 V + \frac{\rho}{\varepsilon} = 0 \quad (1)$$

This calculation was performed using the Delphi module implemented in Discovery Studio 2.5 [8].

2.6. Calculation of binding affinity and QSAR model

For each molecule in the test set, the relative thermodynamic value (ΔΔGcom) was calculated. This calculation was performed using the MM-PB molecular complexation method. Since the Pyl1 ligand was the most active (IC_{50}^{exp} = 0.014 µM), it was chosen as the reference ligand. The models consisted of first correlating the variation in experimental biological activity (pIC_{50}^{exp}) with that of the enthalpy ($\Delta\Delta H_{MM}$) of Molecular Mechanics (gas model) and then doing the same between the variation in experimental biological activity (pIC_{50}^{exp})and the relative variation in free enthalpy of complexation ($\Delta\Delta G_{com}$) (solvent model). pIC_{50}^{exp} was obtained from the following equation:

$$pIC_{50}^{exp} = -\log_{10}\left({IC_{50}}/{10^6}\right) \quad (2)$$

To validate the MM-PB molecular complexation 3D-RQSA model, statistical indicators of the reliability of linear regressions were calculated.

2.7. Pharmacophore generation

The 3D-QSAR pharmacophore generation protocol (PH4) in Discovery Studio [8], based on the Catalyst HypoGen algorithm [13, 14], was used to develop the PH4 model for DHODH inhibition.

3. Results and discussion

3.1. Training and validation sets

Throughout this work, 12 Pylx inhibitors were used for the test set and 4 Pylx inhibitors were used for the validation set, as shown in Table 1. The experimentally determined inhibitory activities are known and come from a single laboratory [7]. The entire series of inhibitors was obtained by variations at two positions, Ar and R, on the pyrrole nucleus skeleton, as shown in Table 2. The maximum experimental inhibitory concentrations (0.014 µM ≤ IC_{50}^{exp} ≤ 1.6 µM) [7] cover a sufficiently wide range of concentrations to allow the construction of a reliable QSAR model (Table 2). The ratio between the sizes of molecules in the test set and validation set remains a critical factor for correct classification, but it is limited by the number of sets of homologous compounds available in the literature [7, 15].

Table 1 Training set (Pyl1-12) and validation set (Pyl13-16) of PDHODH inhibitors [7] used in the preparation of QSAR models of inhibitor binding. The Ar and R groups are numbered in the first part of the Table as #R ≡ group index**.**

<table>
<tr><td colspan="4"> 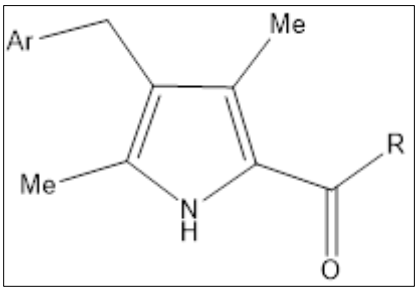 </td></tr>
<tr><td>#R 1</td><td>2</td><td>3</td><td>4</td></tr>
<tr><td> 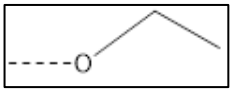 </td><td> 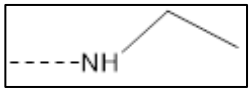 </td><td> 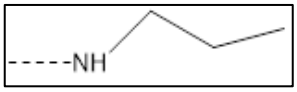 </td><td> 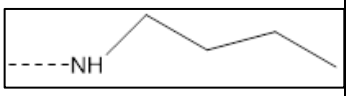 </td></tr>
<tr><td colspan="4">R group</td></tr>
<tr><td>#R 5</td><td>6</td><td>7</td><td>8</td></tr>
<tr><td> 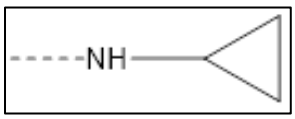 </td><td> 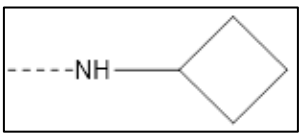 </td><td> 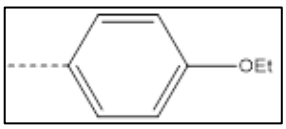 </td><td> 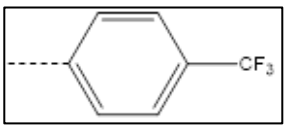 </td></tr>
<tr><td colspan="4">R group</td></tr>
<tr><td>#R 9</td><td>10</td><td>11</td><td>12</td></tr>
<tr><td> 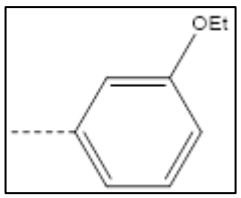 </td><td> 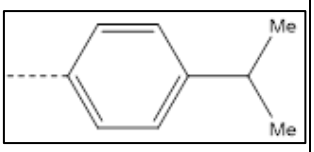 </td><td> 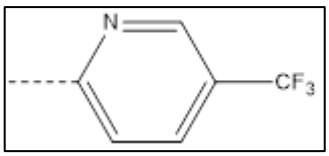 </td><td> 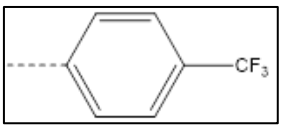 </td></tr>
<tr><td colspan="4">R group</td></tr>
<tr><td>#R 13</td><td>14</td><td></td><td></td></tr>
<tr><td> 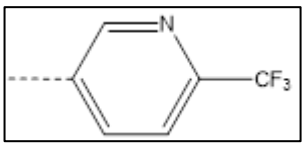 </td><td> 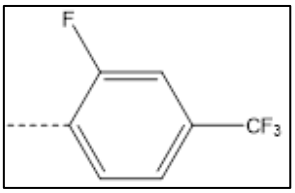 </td><td></td><td></td></tr>
</table>

Table 2. inhibitory activities (IC_{50}^{exp}) of molecules used for the training set (Pyl1-12) and validation set (Pyl13-16)

Training Set	**Pyl 1**	**Pyl 2**	**Pyl 3**	**Pyl 4**
#Ar-#R	8-1	8-2	9-1	13-5
IC_{50}^{exp} (µM)	0.014	0.019	0.021	0.022
Training Set	**Pyl 5**	**Pyl 6**	**Pyl 7**	**Pyl 8**
#Ar-#R	13-3	6	10-1	7-1
IC_{50}^{exp} (µM)	0.031	13-6	0.040	0.045
Training Set	**Pyl 9**	**Pyl 10**	**Pyl 11**	**Pyl 12**
#Ar-#R	12-3	11-1	11-6	2
IC_{50}^{exp} (µM)	0.059	0.036	0.220	12-4
Validation Set	**Pyl 13**	**Pyl 14**	**Pyl 15**	**Pyl 16**
#Ar-#R	12-5	14-1	13-2	13-3
IC_{50}^{exp} (µM)	0.023	0.036	0.036	1.600

3.2. QSAR Model

3.2.1. One Descriptor QSAR Models

The complexation of the 12 inhibitors in the test set and the 4 inhibitors in the validation set was achieved by in situ modification of the crystal structure of complex 1, in this case the first inhibitor in the test set series (DHODH: Pyl1), following the procedure detailed in the Methods section. The relative Gibbs free energy (GFE) of complex formation (DHODH: Pyl) was calculated for each of the 16 optimized (enzyme-inhibitor) complexes. Table 3 presents the calculated energy values and their components. To establish a quantitative structure-activity relationship (QSAR), the experimental inhibitory activities (IC_{50}^{exp}) of the Pylx compounds were converted to (pIC_{50}^{exp}) using the using equation 2. The linear relationship derived from this RQSA model between pIC_{50}^{exp} and $\Delta\Delta G_{com}$ is highlighted in the following equation:

$$pIC_{50}^{exp} = - 0.1207 \times \Delta\Delta G_{com} + 7.8526 \quad (3)$$

The resulting strong correlation confirmed the binding modes of Pylx within the DHODH site, leading to the definition of the DHODH inhibition pharmacophore. In order to better understand the binding affinity of Pylx to DHODH, the gas-phase complexation enthalpy ($\Delta\Delta H_{MM}$) was calculated and analyzed. The statistical significance of this linear relationship (Table 4, Equation A) highlighted the crucial role of inhibitor-enzyme interactions, particularly when solvent effects and entropy loss upon binding to DHODH were neglected. This correlation explained approximately 90% of the variation in values, highlighting the contribution of enthalpy to ligand binding affinity. In addition, a more comprehensive descriptor, the Gibbs free energy (GFE) of the formation of the Pyl1 complex, integrating all key components $\Delta\Delta H_{MM}$, $\Delta\Delta TS_{vib}$ and $\Delta\Delta G_{sol}$, was evaluated (Table 4, equation B). The relatively high correlation coefficient (R^2 = 0.95) demonstrated that structural information derived from 3D models of the complexes (DHODH: Pylx) could reliably predict how pyrrole inhibitors interact within the active site of DHODH using QSAR model B, as shown in Table 3. These values (Table 4) indicate that there is a strong relationship between the bonding model and the experimental model of the pyrrole series.

Table 3 Gibbs free energy (binding affinity) and its components for the training set of DHODH inhibitors Pyl1-12 and validation set inhibitors Pyl13-16 [7]

Training set [a]	**M_W** [b]	**$\Delta\Delta H_{MM}$** [c]	**$\Delta\Delta G_{sol}$** [d]	**$\Delta\Delta TS_{vib}$** [e]	**$\Delta\Delta G_{com}$** [f]	**IC_{50}^{exp}** [g]
	[g.mol^{-1}]	**[kcal.mol^{-1}]**	**[kcal.mol^{-1}]**	**[kcal.mol^{-1}]**	**[kcal.mol^{-1}]**	**[µM]**
Pyl 1	311.299	0.00	0.00	0.00	0.00	0.014
Pyl 2	325.326	1.10	-0.47	-1.38	2.01	0.019
Pyl 3	324.341	2.88	-1.68	0.27	0.93	0.031
Pyl 4	351.366	1.23	0.85	-1.38	3.45	0.036
Pyl 5	285.381	1.24	1.38	0.06	2.55	0.04
Pyl 6	33.34	3.09	0.67	-1.18	4.95	0.022
Pyl 7	287.354	3.32	-0.75	-0.06	2.63	0.045
Pyl 8	326.314	2.28	1.86	0.01	4.13	0.06
Pyl 9	287.354	2.26	2.42	-0.97	5.65	0.021
Pyl 10	338.367	1.34	0.06	-1.99	3.39	0.059
Pyl 11	351.366	7.31	-0.25	-1.81	8.86	0.22
Pyl 12	352.394	16.03	3.24	1.74	1.53	1.8
Validation set [a]	M_W [b]	$\Delta\Delta H_{MM}$ [c]	$\Delta\Delta G_{sol}$ [d]	$\Delta\Delta TS_{vib}$ [e]	$\Delta\Delta G_{com}$ [f]	$pC_{50}^{pre}/pC_{50}^{exp}$ [h]
	[g.mol^{-1}]	[kcal.mol^{-1}]	[kcal.mol-1]	[kcal.mol-1]	[kcal.mol-1]	
Pyl 13	322.325	0.13	2.55	-3.02	5.71	0.94
Pyl 14	329.289	2.44	-0.16	-2.51	2.63	0.99
Pyl 15	325.329	3.11	1.64	-1.49	6.24	0.95
Pyl 16	339.355	5.13	1.29	-1.61	8.86	0.91

[a] for the chemical structures of the training set of inhibitors see Table 1; [b] Mw is the molar mass of inhibitors; [c] $\Delta\Delta H_{MM}$ is the relative enthalpic contribution to the GFE change related to E-I complex formation derived by MM;$\Delta\Delta H_{MM} \approx [E_{MM}\{E\text{-}Ix\} - E_{MM}\{Ix\}] - [E_{MM}\{E\text{-}Iref\} - EMM\{Iref\}]$, Iref is the reference inhibitor Pyl1; [d]ΔΔGsol is the relative solvent effect contribution to the GFE change of E-I complex formation: ΔΔGsol = [Gsol{E-Ix} − Gsol{Ix}] − [Gsol{E-Iref} − Gsol{Iref}]; [e] ΔΔTSvib is the relative entropic contribution of inhibitor to the GFE of E-Ix complex formation: ΔΔTSvib = [TSvib{Ix}E − TSvib{Ix}] − [TSvib{Iref}E − TSvib{Iref}]; [f]ΔΔGcom is the overall relative GFE change of E-Ix complex formation: $\Delta\Delta G_{com} \approx \Delta\Delta H_{MM} + \Delta\Delta G_{sol} - \Delta\Delta TS_{vib}$; [g] IC_{50}^{exp} is the experimental half-maximal inhibition concentration of PfA.M1obtained from ref. [**Error! Bookmark not defined.**]; [h] ratio of predicted and experimental half-maximal inhibition concentrations $pC_{50}^{pre}/pC_{50}^{exp}$ ($pIC_{50}^{pre} = -\log_{10} IC_{50}^{pre}$) was predicted from computed ΔΔGcom using the regression equation for DHODH shown in Table 4, B.

Table 4 Analysis of computed binding affinities $\Delta\Delta G_{com}$, its enthalpic component $\Delta\Delta H_{MM}$, and experimental half-maximal inhibitory concentrations $\mathbf{pIC_{50}^{pre}} = -\log_{10} \mathbf{IC_{50}^{pre}}$ of Pylx towards DHODH [7]

Statistical Data of Linear Regression	**A**	**B**
$pIC_{50}^{exp} = - 0.1263 \times \Delta\Delta H_{MM} + 7.7312$ (A) $pIC_{50}^{exp} = - 0.1207 \times \Delta\Delta G_{com} + 7.8526$ (B)		
Number of compounds n	12	12
Squared correlation coefficient of regression R^2	0.90	0.95
LOO cross-validated squared correlation coefficient R^2_{xv}	0.89	0.94
Standard error of regression σ	0.19	0.14
Statistical significance of regression, Fisher F-test	94.20	184.04
Level of statistical significance α	>95%	>95%
Range of activities IC_{50}^{exp} [μM]	0.014 – 1.6	0.014 – 1.6

The statistical data confirmed validity of the correlation Equations (A) and (B) plotted on Figure 1. The ratio $pC_{50}^{pre}/pC_{50}^{exp} \approx 1$ (the pIC_{50}^{pre} values were estimated using correlation Equation B, Table 4) calculated for the validation set Pyl13-16 documents the substantial predictive power of the complexation QSAR model from Table 2.

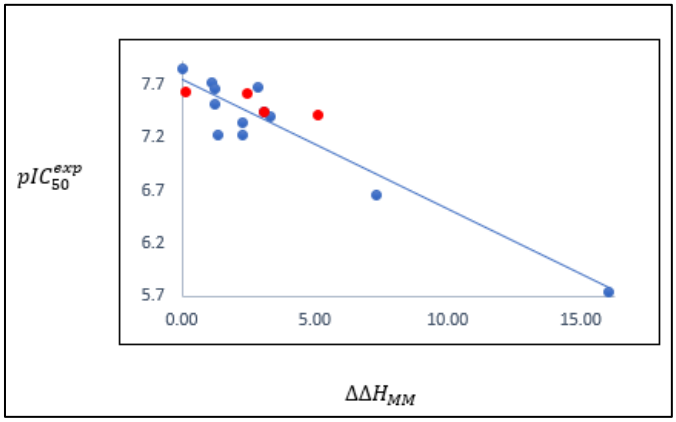

A

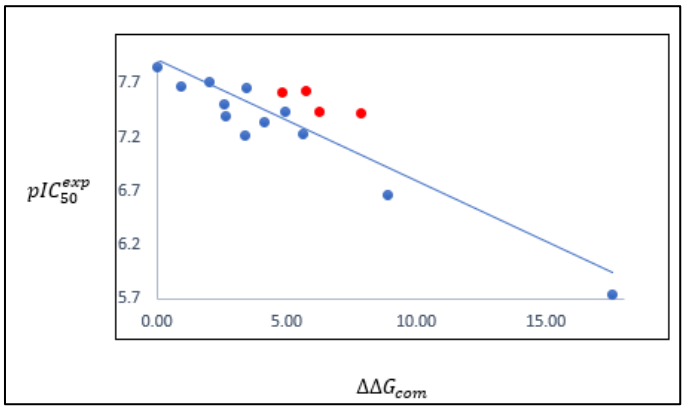

B

Figure 1 (A) plot of correlation equation between $\boldsymbol{pIC_{50}^{exp}}$ and relative enthalpic contribution to the GFE ($\Delta\Delta H_{MM}$ [kcal.mol^{-1}]). (B) similar plot for relative complexation Gibbs free energies of the DHODH-Pyl complex formation $\Delta\Delta G_{com}$ [kcal.mol^{-1}] of the training set [7]. The validation set data points are shown in red color

3.3. Binding Mode of Pyls

Beyond the robustness of the QSAR model, analysis of interactions between Pylx and DHODH active site residues within a radius of 10 Å revealed the key interactions responsible for the affinity of pyrrole inhibitors (Pylx) with DHODH. These interactions were highlighted through the Pyl 1 inhibitor, the most active inhibitor in the test set, as shown in Figure 2. Van der Waals interactions, low-intensity electrical interactions, were observed between Pyl1 and the residues Tyr168, Phe 171, Leu 172, Gly 181, Arg 265, and Gly 535 of DHODH. A T-shaped Pi-Pi stacking interaction, which is attractive and non-covalent, was observed with the Phe168 residue of DHODH. In addition, a Pi-Sulfur interaction was observed between the Cys 175 residue of DHODH and the phenyl ring of Pyl 1. Pi-alkyl interactions were observed between residues His 185, Phe 227, Ile 263, and Tyr 528 of DHODH with Pyl1. Hydrogen interactions were observed in small quantities in almost all complexes. These interactions are important for protein folding, conformational changes, and protein/ligand recognition. On the ligand side, they affect the physicochemical properties of molecules, such as solubility and membrane permeability, which are crucial elements in drug development.

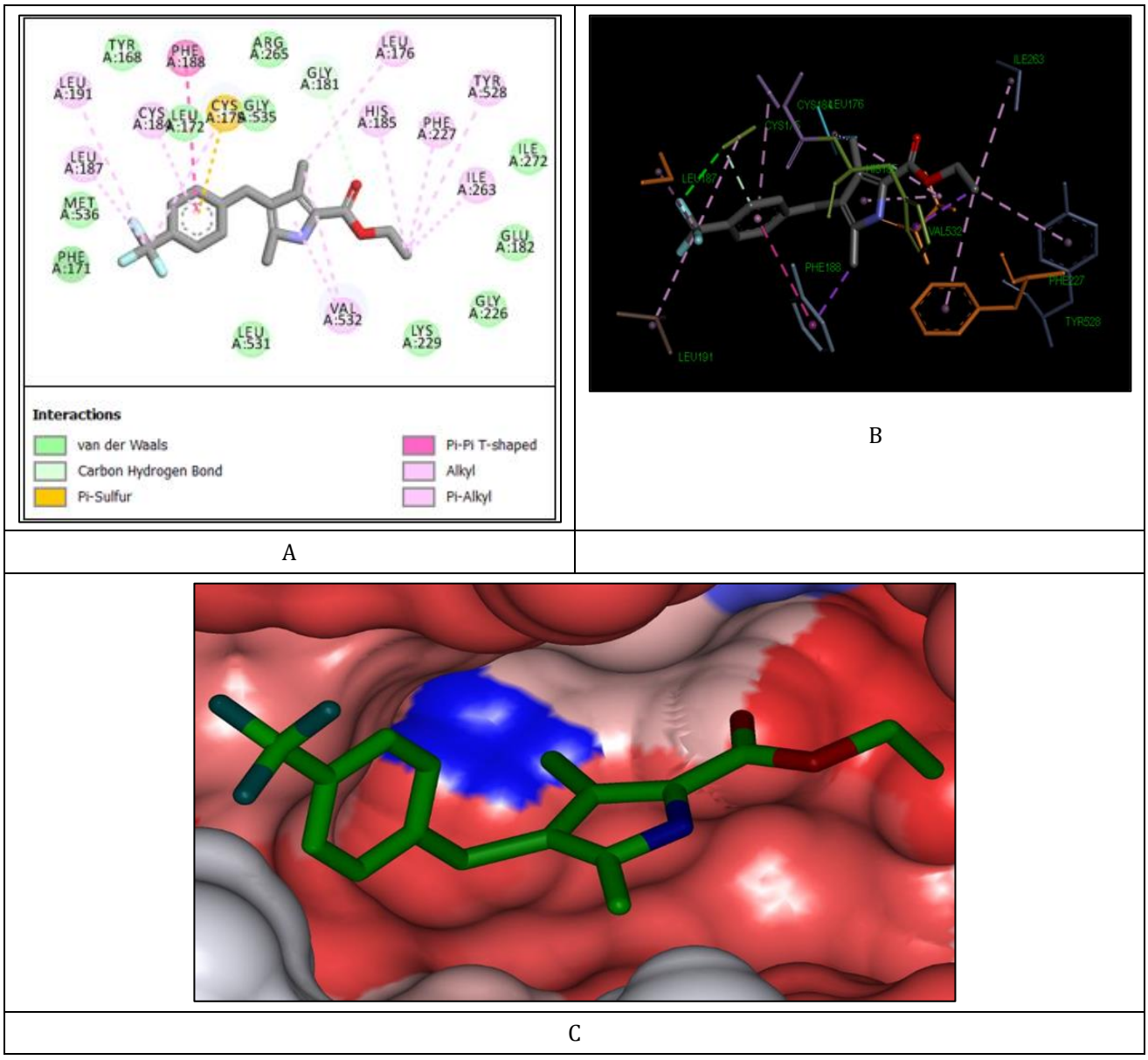

A B C

Figure 2 (A) 2D interaction diagram of the most active inhibitor (Pyl 1) in the training set within the active site of DHODH, (B) Schematic 3D interaction of Pyl 1 at the active site of the DHODH enzyme, (C) Hydrophobic surface of the active site of DHODH. Surface coloring legend: red ≡ hydrophobic, blue ≡ hydrophilic and white ≡ intermediate

3.4. 3D-QSAR Pharmacophore Model

3.4.1. PfA-M1 Active Site Pharmacophore

The interaction generation protocol in Discovery Studio molecular modeling program [8] provides the pharmacophore features of the active site of a protein. DHODH predominantly displays aliphatic and hydrophobic aromatic features at the active site.

3.4.2. Generation and Validation of 3D-QSAR Pharmacophore

A 3D-QSAR pharmacophore model for DHODH inhibition was constructed based on the active conformations of the 12 Pylx inhibitors in the training set (TS) and validated by the 4 inhibitors in the validation set (VS). The 16 pyrrole-derived Pylx inhibitors cover a wide range of experimental activity (0.014 µM - 1.6 µM) (Table 2). The 3D-QSAR pharmacophore generation process is divided into three main phases: the constructive phase (i); the subtractive phase (ii); and finally, the optimization phase (iii). The hypotheses were scored based on errors in the activities estimated from regression and complexity using a simulated annealing approach. At the end of the optimization, the 10 highest-scoring unique pharmacophore hypotheses were retained, all displaying three characteristics: cost values, correlation coefficients, and mean squared deviation values (RMSD). The pharmacophore characteristics and maximum fit values of the 10 highest-ranked hypotheses (Hypo1-Hypo10) are shown in Table 5. They were selected based on significant parameters, such as a high correlation coefficient, low total cost, and low RMSD. Their selection was based on significant statistical parameters, including a high correlation coefficient, low total cost, and low RMSD. The cost difference (Δ = 184.5171) was calculated as follows: zero cost (216.723) – fixed cost (32.2059), indicating a high probability (> 90%) that the model represents a true correlation. Standard parameters such as RMSD vary between 1.72 and 4.46, and the correlation coefficient squared (R^2) ranges from 0.96 to 0.63. The first hypothesis of PH4 was selected for further analysis. Its evaluation consisted of mapping the most active ligand, Pyl1, from the set of 12 inhibitors in the test set (Figure 3, B), showing its active conformation with the Hypo1 pharmacophore for DHODH inhibition. The statistical data for all hypotheses (costs, RMSD, R^2) are listed in Table 5. The linear correlation equation of the 3D-QSAR pharmacophore model explaining the variation in experimental biological activity as a function of predicted activity is given by the following linear relationship:

$$\mathrm{pIC}_{50}^{\mathrm{exp}} = 1.1585 \times \mathrm{pIC}_{50}^{\mathrm{pred}} - 1.1488 \quad (4)$$

This relationship is illustrated in Figure 4E with its internal validation reliability statistical parameters such as n = 12, R^2= 0.93, R^2_{XV} = 0.91, F-test = 123.43, α = 0.16 < 1, with a confidence level of 95%. These results indicate that the 3D-QSAR pharmacophore model is highly reliable and can be used to search for new competitive analogues for DHODH inhibition.

Table 5 Parameters of 10 generated PH4 pharmacophoric hypotheses for DHODH inhibitor after Cat-Scramble validation procedure (49 scrambled runs for each hypothesis at the selected level of confidence of 98%)

Hypothesis	RMSD [a]	R^2 [b]	Total Costs [c]	Costs Difference [d]	Closest Random [e]
Hypo1	1.72	0.96	63.10	153.61	45.79
Hypo2	2.21	0.92	64.09	152.62	50.47
Hypo3	2.79	0.87	82.42	134.29	52.706
Hypo4	3.73	0.76	121.82	94.90	53.47
Hypo5	3.78	0.75	124.22	92.50	54.77
Hypo6	3.81	0.75	130.66	86.06	57.87
Hypo7	4.00	0.71	131.23	85.48	58.38
Hypo8	4.10	0.70	136.05	80.67	62.63
Hypo9	4.13	0.69	137.04	79.67	66.84
Hypo10	4.45	0.63	160.47	56.24	67.66

a root means square deviation; b squared correlation coefficient; c overall cost parameter of the PH4 pharmacophore; d cost difference between Null cost and hypothesis total cost; e lowest cost from 49 scrambled runs at a selected level of confidence of 98%, the Configuration cost = 9.85.

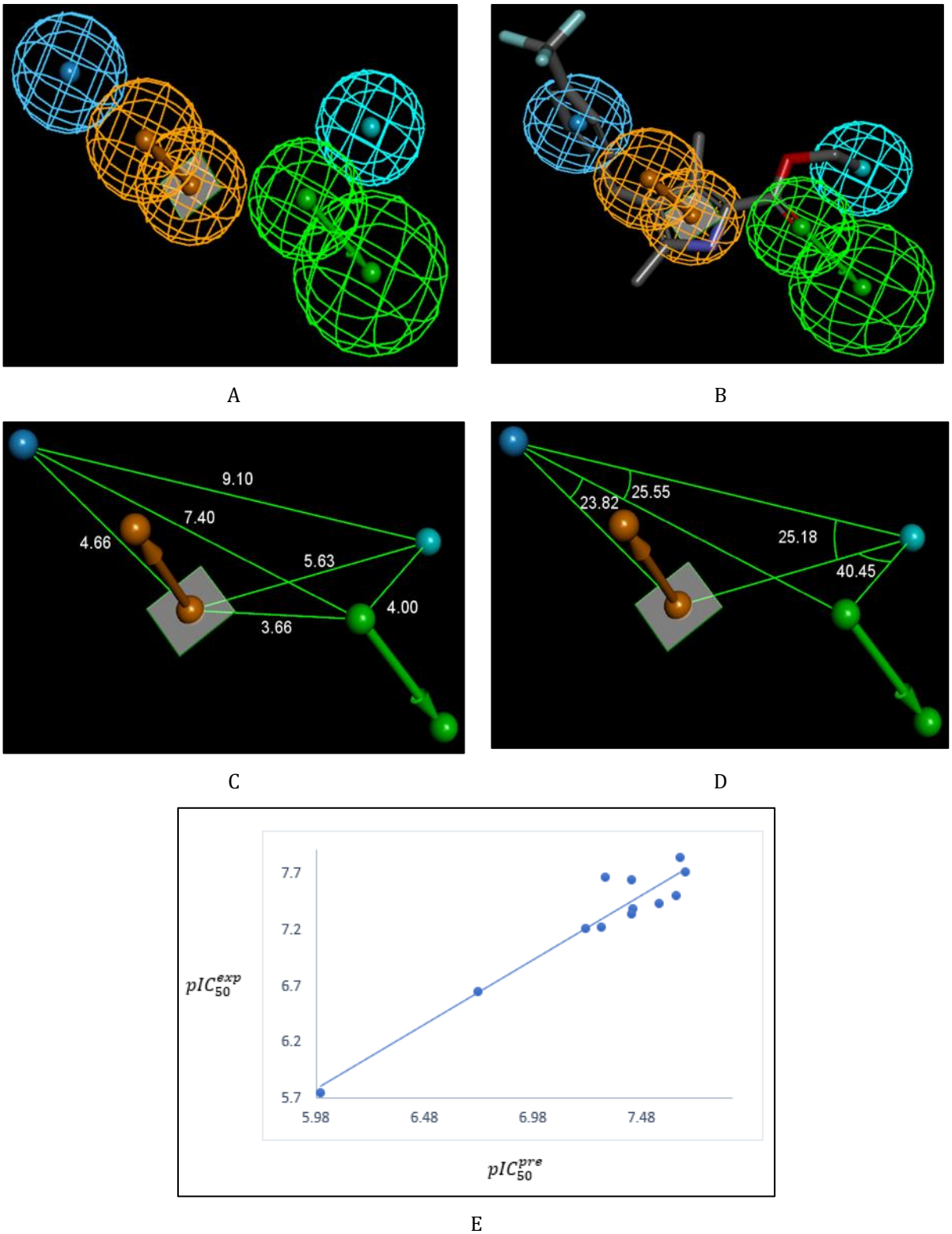

Figure 3 (A) Features coordinates of centers, (B) mapping of pharmacophore of DHODH inhibitor with the most potent molecule Pyl1, Feature legend: HYDA = Hydrophobic Aliphatic (blue), HYD = Hydrophobic (cyan), HBA = Hydrogen bond Acceptor (green), aromatic cycle (orange), (C) distances between centers, (D) angles between centers of pharmacophoric features, (E) correlation plot of experimental vs. predicted inhibitory activity

Abbreviations

- 2D: Two-dimensional;
- 3D: Three-dimensional;
- CACC: Computer-Aided Combinatorial Chemistry;
- CADD : Computer-Aided Drug Design;
- CFF: Consistent Force Field;
- DHODH: Dihydroorotate dehydrogenase;
- $\Delta\Delta G_{com}$: Relative complexation GFE;
- GFE: Gibbs free energy;
- ΔΔGsol: Relative solvation GFE;
- HBA: Hydrogen bond Acceptor;
- HBD: Hydrogen bond Donor;
- H_{MM}: Enthalpy component of GFE;
- HYD: Hydrophobic;
- HYDA: Hydrophobic Aliphatic;
- IC_{50}^{exp}: Inhibitory concentration;
- MM: Molecular mechanics;
- MM-PB: Molecular mechanics–Poisson–Boltzmann;
- PDB: Protein Data Bank;
- Pyl: Pyrrole;
- Pylx: Training set and Validation set of Pyrrole;
- Pf: plasmodium falciparum;
- PH4: Pharmacophore;
- QSAR: Quantitative structure–activity relationships;
- RMSD: Root-mean square deviation;
- SAR: Structure–activity relationships;
- TS: Training set;
- VS: Validation set;
- WHO: World Health Organization

4. Conclusion

This work is part of an effort to understand and analyze how pyrrole inhibitors bind to the DHODH site using physics-based simulation methods. The specific objective of this work is very important, given the emergence of multi-resistant and ultra-resistant strains to the drugs available for malaria control. This work initially led us to establish a correlation between the enthalpy of formation of the DHODH: Pylx complex in gas with the inhibitory activity of DHODH using molecular mechanics. We then took into account the effect of solvation according to the Poisson-Boltzmann model to illustrate the conditions of the biological environment and finally introduced a contribution relating to the loss of entropy of the ligand vibration at the active site of the enzyme (DHODH). The combination of these three terms constitutes the free enthalpy of formation of the complex, and enabled us to achieve a QSAR model that is closer to experimental reality. Indeed, it explains nearly 95% of the variation in inhibitory activity by the variation in the free enthalpy of formation of the DHODH: Pylx complex. Next, we generated a pharmacophore, a typical model of pyrrole-derived molecule inhibitors. We started with a series of 16 inhibitors derived from the pyrrole nucleus to build the QSAR model of DHODH inhibition. The QSAR equations obtained enabled us to understand how inhibitors bind within the active site of DHODH and to analyze the various interactions resulting from this binding mode. Furthermore, the pharmacophore model found enabled us to identify the nature of the chemical groups that enhance activity. This physics-based simulation study could be recommended in the context of synthesis and biological evaluation to identify new antimalarial molecules with a good pharmacokinetic profile that can be administered orally.

Compliance with ethical standards

Disclosure of conflict of interest

No conflict of interest to be disclosed.

References

[1] Gaudilliere Jean-Paul, « Professional or Industrial Ordre? Patents, Biological Drugs, and Pharmaceutical Capitalism in Early Twentieth Century Germany », History and Technology, n° 2, 2008.

[2] Niaré A, N'Guessan H, Dali B, Megnassan E. Computer-assisted design of hydroxamic acid derivatives inhibitors of M1 Metallo Aminopeptidase of Plasmodium falciparum with favorable pharmacokinetic profile. J Pharm Res Int, vol. 34, p. 21–44, 2022.

[3] World malaria report 2021. Geneva, World Health Organization. Licence : CCBY-NC-SA 3.0 IGO https://apps.who.int/iris/handle/10665/350147, 2021.

[4] K. Kannan Sivaraman, A. Paiardini, M. Sienczyk, C. Ruggeri, C. A. Oellig, J. P. Dalton, P. J. Scammells, M. Drag et S. McGowan, «Synthesis and structure–activity relationships of phosphonic arginine mimetics as inhibitors of the M1 and M17 aminopeptidases from Plasmodium falciparum.,» J. Med. Chem., vol. 56, p. 5213–5217, 2013.

[5] Niaré A., Alex, A.Y.Z., Bernard, D.A.M., Marius, K.S., Stéphane, D.S., Moise, K.A., Guy-Richard, K.M., Fagnidi, Y.K.H., Doh, S. Study by Molecular Docking of the Interactions Between Dihydroorotate Dehydrogenase and a Series of Inhibitors of Pyrrole Derivatives for the Treatment of Malaria. Asian Journal of Chemical Sciences, vol. 15, p. 92–110, 2025.

[6] V.K. Vyas and M. Ghate. Recent Developments in the Medicinal Chemistry and TherapeuticPotential of Dihydroorotate Dehydrogenase (DHODH) Inhibitors. Minireviews in Medicinal Chemistry, vol. 11, p. 1039–1055, 2011.

[7] Sreekanth Kokkonda, Xiaoyi Deng, Karen L. White, Farah El Mazouni, John White, David M. Shackleford. Lead Optimization of a Pyrrole-Based Dihydroorotate Dehydrogenase Inhibitor Series for the Treatment of Malaria. J. Med. Chem., vol. 63, p. 4929–4956, 2020.

[8] Discovery Studio molecular modeling and simulation program, Version 2.5, Accelrys, Inc., San Diego, CA, 2009.

[9] Insight-II et Discover Molecular Modeling and Simulation Package, version 2005; Accelrys: San Diego, CA, États-Unis, 2005.

[10] Rika J. Kouadja, Logbo M. Mousse, Koffi C. Kouman, Mama Nsangou, Eugene Megnassan.Computer-Assisted Design of Benzoisoxazol derivatives Inhibitors of Bromodomain- containing Protein 4 (BRD4) with Favorable Pharmacokinetic Profile. Int. J. Pharm. Sci. Drug, vol. 15, p. 47–64, 2023.

[11] Soro I, N'Guessan H, Abou A, N'Guessan R K, Megnassan E. Conformational study of molecules in a biological environment, design of inhibitors of human aminopeptidase M1 implicated in cancer therapy. Universal Journal of Pharmaceutical Research.in our previous studies on the design of inhibitors. Universal J. of Pharm Research, vol. 8, p. 71–86, 2023.

[12] Gilson, Michael K. and Barry H. The inclusion of electrostatic hydration energies in molecular mechanics calculations, J. Comput. Aided Mol. Des., vol. 5, p. 5–20, 1991.

[13] Wang X, Xu Y, Zheng H, Yu K. An Extendible, Graph-Neural-Network-Based Approach for Accurate Force Field Development of Large Flexible Organic Molecules. arXiv preprint arXiv:2106.00927, 2021.

[14] Niaré, A., N'guessan, A.-B., Djako, B. A. M., Dembélé, G. S., Koné, M. G.-R., Yéo, Y. (2024). QSAR, pharmacophore, and molecular docking studies for the design of novel arylamide-derived inhibitors of Mycobacterium tuberculosis. Chemical Science International Journal, vol. 33, p. 212–224, 2024.

[15] Djako, A. M. B., Niaré. A., Fofana. I., Moussé. L. M., Kéita. M., Megnassan. E. Identification of Novel Polyketide Synthase 13 of Mycobacterium Tuberculosis Inhibitors: A Modelling Approach Using the Pharmacophore Method -Based Virtual Screening. Journal of Advances in Medical and Pharmaceutical Sciences. vol. 27, p. 1–18, 2025.